

# Ductile particle ceramic matrix composites—Scientific curiosities or engineering materials?

J.A. Yeomans\*

*Faculty of Engineering and Physical Sciences, University of Surrey, Guildford,  
Surrey GU2 7XH, United Kingdom*

Available online 29 January 2008

## Abstract

This review is concerned with ductile particle ceramic matrix composites, which are a group of materials comprising micro- or nano-scale metallic particles in a ceramic matrix. The most studied materials have an alumina matrix; nickel, iron, molybdenum, copper, and silver are some of the more frequently used metals. In contrast to conventional cermets and composites containing an interconnected metallic phase, the particles are discrete. The larger particles provide a toughening increment by deforming plastically and bridging an advancing crack. For the nanoscale composites significant improvements in strength have been reported. Improvements in strength and toughness, coupled with changes to elastic properties and thermal conductivity, have led to improved thermal shock resistance and a consideration of these materials for wear applications.

© 2007 Elsevier Ltd. All rights reserved.

*Keywords:* Composites; Microstructure-final; Toughness and toughening; Thermal shock resistance; Wear resistance

## 1. Introduction

There are a host of materials which comprise metallic inclusions essentially either within or on a ceramic matrix; however, the term ‘ductile particle ceramic matrix composite’ is usually taken to mean a material that has been designed such that the metal is in the form of inclusions that are isolated from each other (rather than forming a continuous network) and which deform plastically, thereby producing a toughening increment. Although there are earlier examples of such composites (e.g., tungsten in glass,<sup>1</sup> molybdenum in alumina,<sup>2</sup> iron, cobalt and nickel in magnesia,<sup>3,4</sup> and nickel and aluminium in glass,<sup>5,6</sup>) an increasing interest in this group of materials developed in the late 1980s and early 1990s, a period during which a number of allied topics were being explored. There was considerable effort being directed towards producing tougher ceramics and a whole range of ceramic matrix composites (CMCs), principally based on continuous ceramic fibres, were being developed. Alongside this there was the development of CMCs produced by directed metal oxidation, which tended to give materials with a continuous or partially continuous network of a metallic phase.

When a particulate second phase is introduced into a brittle matrix, there are several toughening mechanisms that may operate but the maximum benefit is derived from metallic particles if they are able to deform plastically and bridge an advancing crack (see Fig. 1). This is easier to achieve in systems in which the metallic phase is (partially) continuous e.g. ‘traditional’ cermets such as tungsten carbide–cobalt and the directed metal oxidation products. However, it is not always desirable to have an interconnected metallic phase, hence the development of composites containing discrete metallic particles. The mechanism of ductile particle bridging is a crack wake effect with an associated process zone so these composites would be expected to show resistance-curve (*R*-curve) behaviour. At steady state, the toughening increment,  $\Delta G_c$ , is given as

$$\Delta G_c = V_f \int_0^{u^*} \sigma(u) du \quad (1)$$

where  $V_f$  is the area fraction of ductile particles intersected by the crack plane (usually taken to be equal to the volume fraction of ductile particles),  $\sigma(u)$  is the stress/stretch relationship for the metallic particle, and  $u^*$  is the crack opening displacement when the metallic particle fails. Scaling the nominal stress,  $\sigma$ , with the yield stress,  $\sigma_y$ , and the displacement,  $u$ , with a characteristic

\* Tel.: +44 1483 689613; fax: +44 1483 686291.  
E-mail address: [j.yeomans@surrey.ac.uk](mailto:j.yeomans@surrey.ac.uk).

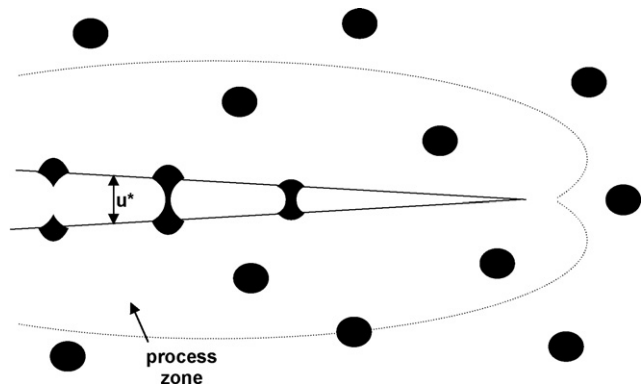


Fig. 1. Schematic diagram of ductile particles bridging an advancing crack.

dimension of the metallic phase,  $r$ , gives:

$$\Delta G_c = \chi V_f \sigma_y r \quad (2)$$

where  $\chi$  is the ‘work-of-rupture’ parameter, which depends on the ductility and work hardening coefficient of the metallic phase and the degree of constraint, and is given by

$$\chi = V_f \int_0^{u^*/r} \frac{\sigma(u)}{\sigma_y} d\frac{u}{r} \quad (3)$$

From experiments on lead wires in glass,<sup>7</sup> values for  $\chi$  are expected to range from 1 to 6, with the higher values being associated with greater degrees of particle–matrix debonding or matrix fracture (see Fig. 2).

Thus, the ideal ductile particle CMC comprises metallic particles within a ceramic matrix such that an advancing crack is attracted to a particle. That particle then debonds partially from the matrix, ideally to its polar regions, and deforms plastically, thus absorbing energy and bridging the crack, providing closure tractions, both of which will provide a toughening increment. However, putting this concept into practice poses several challenges and has resulted in a wide range of materials with some interesting properties. This brief review will consider some micro- and nano-scale ductile particle CMCs, concentrating on the toughening increments achieved, before considering other properties, principally thermal shock and wear resistance, and concluding with an outlook for these materials.

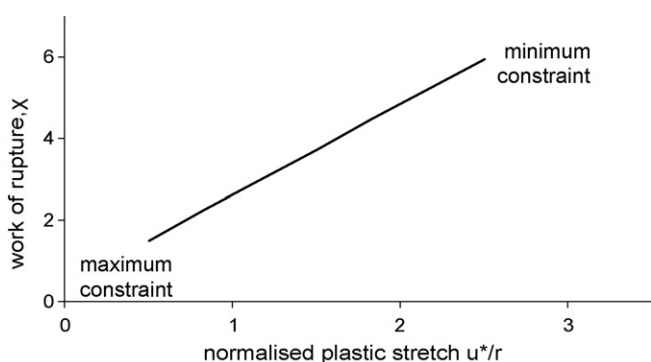


Fig. 2. Work of rupture parameter as a function of plastic deformation of the metallic phase (adapted from Ref. [7]).

## 2. Micro-scale ductile particle ceramic matrix composites

For an advancing crack to be attracted to an inclusion, rather than repelled by it, the elastic modulus of the inclusion must be lower than that of the matrix; clearly this is not a problem for most engineering ceramic/metal combinations. From Eq. (1), the toughening increment should increase with the volume fraction of metal particles. There is, however, a limit to the amount of metallic phase that can be added if the particles are to remain isolated from each other and hence contribute effectively to the toughening. Further, interconnected metallic particles are likely to lead to adverse changes in some properties, such as electrical insulation, corrosion resistance, and creep performance. For example, it has been observed that particle contents over 20 vol% can lead to a substantial increase in the electrical conductivity of the composite.<sup>8</sup> Further, the toughening increment should increase with the yield strength of the metal and with the size of the inclusion. However, if the inclusion becomes too large then the difference in the coefficients of thermal expansion of the metal and the ceramic matrix is likely to result in cracking, which may lead to an advancing crack being able to by-pass the particle.

Most of the work on micro-scale composites has been concerned with alumina matrices, although other systems have been investigated, including glass (with Mo and/or V particles,<sup>9</sup> Cu particles<sup>10</sup> and Kovar<sup>11</sup>), glass-ceramics (with Ag<sup>12</sup> and Ti<sup>13</sup>), hydroxyapatite (with Ag<sup>14</sup>), and mullite (with Mo<sup>15</sup>). With alumina, nickel,<sup>16–24</sup> silver,<sup>25–29</sup> molybdenum,<sup>30–32</sup> copper,<sup>33,34</sup> iron<sup>35–37</sup> and to a lesser extent niobium,<sup>32,38</sup> chromium,<sup>39</sup> and chromium–nickel<sup>39</sup> alloys were popular choices for the metal inclusions, as they offered the dual benefits of favourable properties and compatibility with the matrix.

Conceptually, the simplest way to produce ductile particle CMCs is to blend the two component powders, i.e. the ceramic and the metal and then compact and sinter (in a reducing atmosphere to prevent oxidation of the metal) or to hot press the blend. Although this method has been used successfully, there are several problems to be overcome in terms of producing a dense, homogenous composite with discrete particles. Hence other methods have been investigated including sol–gel,<sup>18,19</sup> gas reduction, e.g.<sup>17,22</sup> (i.e. incorporating the metal as an oxide and reducing it in situ) and reaction sintering, e.g.<sup>17</sup> Regardless of the processing method chosen, a major challenge is to control the strength of the metal–ceramic bond and hence the degree of debonding. If the bond is too strong then there will be no debonding and the particle will be almost fully constrained, giving little opportunity for plastic stretching. However, if the bond is too weak then the particle will debond from the matrix completely and the crack will by-pass the particle and the only toughening that can be achieved would be that associated with crack deflection, which does not have the same potential for large increases as plastic deformation. One way to circumnavigate the problem of the strength of the interface is to produce metallic particles that are mechanically interlocked with the matrix (see Fig. 3). This can be achieved by carefully controlling the oxygen partial pressure during processing in order to ensure it

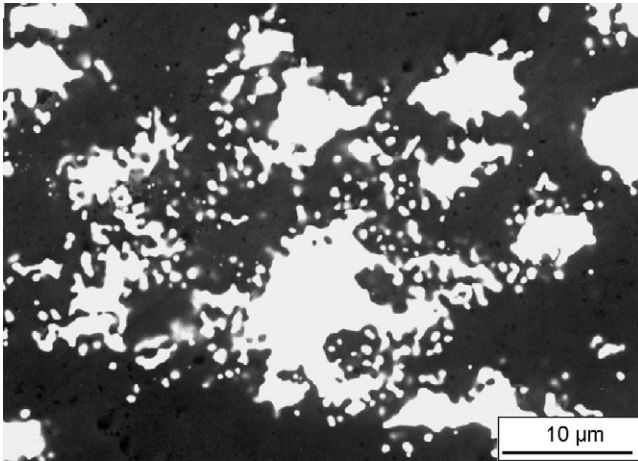


Fig. 3. Scanning electron micrograph of an alumina –20 vol% nickel ductile particle CMC in which the processing conditions have been controlled to produce irregularly shaped nickel particles which are mechanically interlocked with the matrix (courtesy of Xudong Sun).

is sufficiently high at the start of the process that the metal wets the alumina matrix but that it drops in the later stages so that any nickel aluminate that has formed is reduced to nickel and alumina.<sup>23</sup>

Even if the crack does not by-pass the metallic particle, it is not certain that ‘classical’ deformation of the particle to form a neck prior to rupture will occur. Although this has been observed in a limited number of cases (see Fig. 4a and b for examples of approximations to this behaviour), it is more usual for only partial deformation to take place (Fig. 4c) before some other failure mechanism, such as interface failure occurs. Further, embrittlement of the metal can occur during processing such that it cleaves rather than ruptures.

For the full toughening potential of the metallic particles to be realised the crack would have to meet the particle in the middle such the maximum volume of metal was available for deformation. Also, the particle would need to debond to its poles to give the maximum gauge length. This would correspond to a  $u^*/r$  value of 0.5 and hence an approximate value of  $\chi = 1.2$  (from the data given in Ref. [7]). Clearly, this scenario is unrealistic in that if a particle debonds from the matrix to that extent then it is likely to be pulled out of its socket rather than deform. A more realistic value upper bound is  $u^*/r = 0.25$  which gives a value of  $\chi = 0.6$ , which can be used with Eq. (2) to estimate the maximum toughening increment. However, this equation assumes that the particles are all the same size, whereas in practice a size distribution is more likely and using a mean value can lead to incorrect estimations, especially if there is a fairly wide particle size distribution.<sup>40</sup> Taking these factors into account, the increase in fracture toughness that might be achieved in an alumina –20 vol% nickel composite was calculated. The mean particle size was 1.6  $\mu\text{m}$  but the effective particle size was calculated as 6.3  $\mu\text{m}$ , giving almost a factor of four difference in the predicted toughening increment. For this specific composite, the maximum fracture toughness was calculated to be  $\sim 8.4 \text{ MPa m}^{1/2}$ ; an actual fracture toughness of  $7.5 \text{ MPa m}^{1/2}$  was measured using a double cantilever beam method, indicating

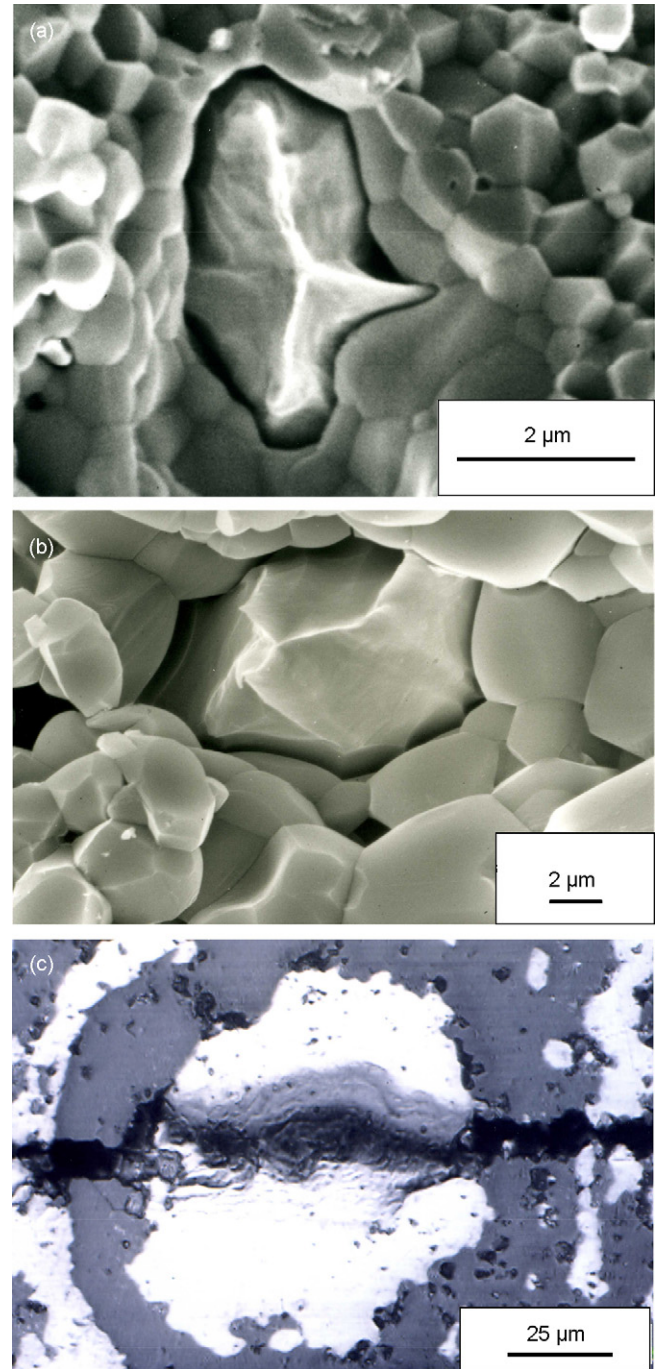


Fig. 4. Examples of metallic particles in alumina matrices (a) scanning electron micrograph showing the necking of a nickel particle (courtesy of Xudong Sun), (b) scanning electron micrograph showing the necking of an iron particle (courtesy of Matthew Aldridge), and (c) extended focus confocal scanning laser micrograph of limited plastic deformation of an iron particle (courtesy of Paul Trusty).

that a significant fraction of the potential toughening increment had been realised. It should be noted that the estimate is very much an upper bound since it is highly unlikely that all of the particles will interact with the crack to achieve the full toughening potential.

Many authors quote fracture toughness values in the region of  $3\text{--}9 \text{ MPa m}^{1/2}$ , which equate to ratios of fracture toughness

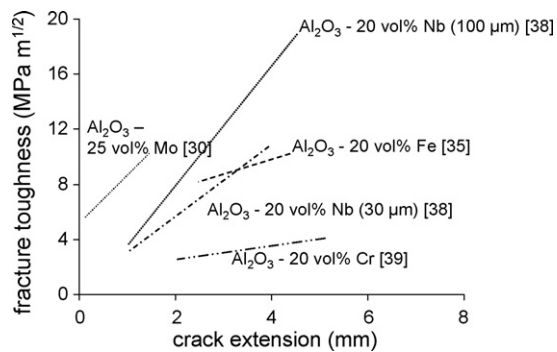


Fig. 5. Compilation of  $R$ -curve behaviour measured for a number of different ductile particle CMCs; the data are taken from the references in parentheses.

of the composite to that of the monolithic matrix in the range slightly over 1–3. Most of these values have been derived from indentation crack lengths. However, as mentioned previously, these composites would be expected to show  $R$ -curve behaviour. When  $R$ -curves are provided, it is clear that considerable crack lengths are needed to achieve the higher levels of toughness and even then the full potential of the ductile particles is not being exploited in many cases (see Fig. 5).

There have been attempts to add two types of second phase particles in the anticipation that there will be some synergy between the toughening mechanisms. Thus, both silver and zirconia have been added to alumina.<sup>41–44</sup> In the work of Tuan and Chen,<sup>41–43</sup> although an increase in toughness was achieved, in the early studies the toughening increment was less than the sum of the increments expected for the two mechanisms acting separately. In the composite containing both toughening agents the zirconia particles failed to transform, as the silver inclusions, which were embedded in the zirconia aggregates, absorbed the transformation stresses. Subsequent improvements in the processing to avoid the formation of zirconia aggregates did result in composites in which the two toughening increments were additive but there was no further increase.

### 3. Nanocomposites

Although improvements in toughness were achieved in the micro-scale ductile particle CMCs, many of the composites had low strengths, partially due to the weak bonding between the inclusions and the matrix, which increased the critical flaw size. In the early 1990s, Niihara<sup>45</sup> and co-workers reported that very high strengths could be achieved by incorporating nanometre-sized ceramic (silicon carbide) particles in ceramic (alumina) matrices to produce nanocomposites. This led to attempts to make ductile particle CMCs with much reduced particle sizes. It was envisaged that it might be possible to development ceramic–metal nanocomposites which would show improved fracture strength and fracture toughness simultaneously by combining the “nanocomposite effect” with the ductility of the metallic phase, although it should have been recognised that the amount of crack bridging that is possible for a very fine scale

metal particle is extremely limited. Again, alumina is the most common matrix and the various metals that have been incorporated into alumina include Ni,<sup>46–53</sup> Mo,<sup>54–56</sup> W,<sup>57,58</sup> Fe,<sup>59,60</sup> Cr,<sup>60–63</sup> Cu,<sup>64,65</sup> and Ni–Co.<sup>66,67</sup>

Alumina–metal nanocomposites can be produced by hot pressing powder blends of either alumina and metal powders or alumina and metal oxide powders. In the later case, reduction of the oxide usually takes place in situ. However, it is always difficult to achieve full density whilst maintaining the nanoscale nature of the metallic phase. These problems, coupled with the health and safety concerns of using very fine powders has led to the development of other methods, many of which use colloidal processing. These have been reviewed recently by Kaplan and Avishai.<sup>68</sup>

The different processing routes lead to different microstructures and in particular the ratio of intra- to inter-granular metallic particles. The very fine scale metallic particles pin the matrix grain boundaries and result in composites which have finer grain sizes than the monolithic matrix material would have if processed under the same conditions. Hence, when trying to assess the benefits of incorporating nanoscale metallic particles in ceramic matrices, it is important to compare materials with comparable grain sizes. Indeed, in some instances, the increase in strength has been attributed to the grain size effect, e.g.<sup>62</sup>

Although composites containing relatively high amounts of nanoscale metallic particles have been reported, in general only a relatively small addition is required to produce a significant improvement in strength. For example, the flexural strength of an alumina was increased from  $\sim 320$  MPa to over 700 MPa through the inclusion of 0.69 vol% of ( $<100$  nm) molybdenum particles (and the fracture toughness was increased from 4 to 6.3 MPa m<sup>1/2</sup>).<sup>56</sup> Data for some examples of composites containing 5 vol% metallic nanoparticles are given in Table 1. In each case, the value for the parent alumina is included to enable comparison and the data are as reported, i.e. without consideration of grain size refinement.

In addition to the increase in strength, there are reports of a change in fracture mode from inter-granular in monolithic alumina to transgranular in alumina–metal nanocomposites, as

Table 1  
Data for alumina–5 vol% metal nanocomposites

Material	Strength (MPa)	Fracture toughness (MPa m <sup>1/2</sup> )	Reference
Al <sub>2</sub> O <sub>3</sub>	536	3.6	65
Al <sub>2</sub> O <sub>3</sub> –5 vol% Cu	953	4.8	
Al <sub>2</sub> O <sub>3</sub>	475	3.6	62
Al <sub>2</sub> O <sub>3</sub> – 5 vol% Cr	736	4.0	
Al <sub>2</sub> O <sub>3</sub>	683	3.5	46
Al <sub>2</sub> O <sub>3</sub> –5 vol% Ni	1090	3.5	
Al <sub>2</sub> O <sub>3</sub>	390	3.6	48
Al <sub>2</sub> O <sub>3</sub> –5 vol% Ni	526	4.2	
Al <sub>2</sub> O <sub>3</sub>	420	3.3	51
Al <sub>2</sub> O <sub>3</sub> –5 vol% Ni	530	5.2	
Al <sub>2</sub> O <sub>3</sub>	528	3.2	57
Al <sub>2</sub> O <sub>3</sub> –5 vol% W	645	3.8	

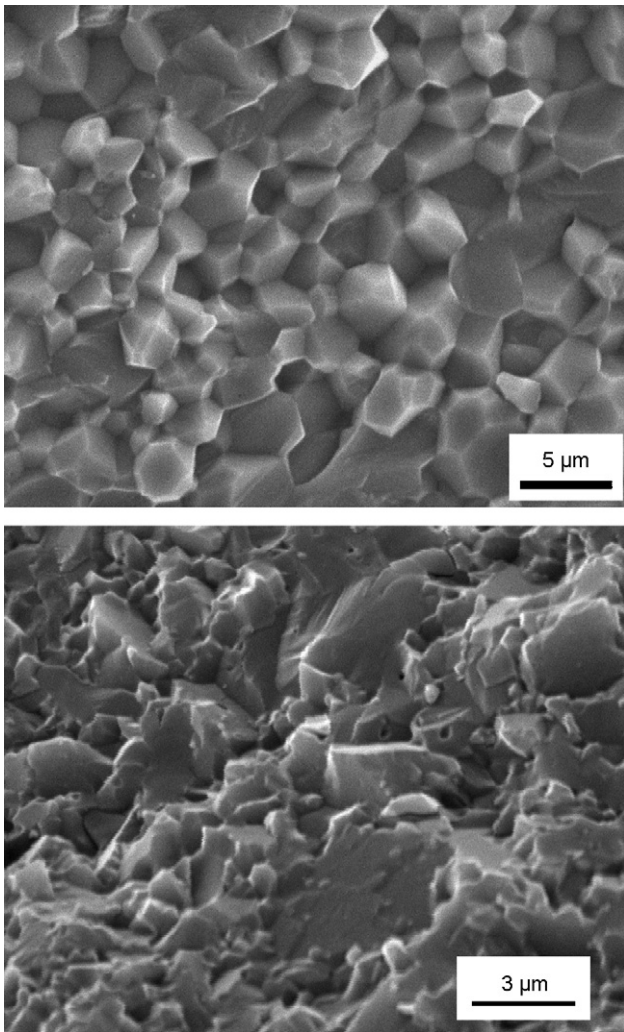


Fig. 6. Scanning electron micrographs of (a) inter-granular fracture surface of alumina and (b) transgranular fracture surface of alumina–5 vol% chromium nanocomposite (reprinted from <sup>62</sup> with permission from Elsevier).

shown in Fig. 6 for an alumina–5 vol% chromium nanocomposite. The reasons for this change in fracture mode and the increased strengths, when they are above the increases that would be expected from grain size refinement, are not clear although the residual stresses resulting from a difference in coefficient of thermal expansion between the nanoparticles and the matrix have been suggested. Interestingly, in the alumina–chromium system the metal has a coefficient of thermal expansion which is less than the alumina (as is the case in alumina–silicon carbide composites) whereas in most systems the metal has a larger coefficient of thermal expansion and the stress states are the reverse of those found in alumina–silicon carbide, i.e. the metal exerts compressive hoop stresses and radial tensile stresses.

#### 4. Wear and thermal shock resistance

As well as potentially providing improvements in toughness and/or strength, adding metallic particles to a ceramic matrix

produces changes to other properties. In general, the metallic phase is softer and less stiff than the matrix hence the composites tend to show reduced hardness and Young's modulus. Also, metals tend to be better conductors of heat than ceramics and thus there is the expectation that the composites will have higher thermal conductivities than the parent matrix materials. Studies on alumina–nickel<sup>24</sup> and alumina–silver<sup>27</sup> show that thermal conductivity is higher for the composite than the matrix material, provided that the particles are sufficiently large that their contribution outweighs the negative effect of the increased interfacial area; the critical sizes were determined to be  $\sim 1.4 \mu\text{m}$  for nickel and  $2.7 \mu\text{m}$  for silver.

Improvements in mechanical properties and thermal conductivity might be expected to be of benefit in wear situations. Alumina containing silver particles has been used as a cutting tool in laboratory tests on a plain carbon steel.<sup>29</sup> The performance of the research material was broadly comparable with that of a commercially available zirconia toughened alumina material.

In a recent study, the abrasive wear behaviour of alumina–molybdenum and alumina–niobium composites has been evaluated.<sup>32</sup> The composites were formed into pins and abraded against a tungsten carbide–cobalt disc. The alumina–niobium composites were more wear resistant than the alumina–molybdenum ones and reported as being comparable with the parent alumina. This was attributed to the stronger bonding and closer matching of the coefficients of thermal expansion between alumina and niobium. However, the cermet discs were worn significantly by the alumina–niobium composites but not by the alumina–molybdenum ones. Thus, these studies indicate that there is further work to do in evaluating and understanding wear behaviour and optimising composites before commercial applications will be viable.

The thermal shock resistance of ductile particle CMCs can be superior to that of the monolithic matrix material. Typically when a dense engineering ceramic is quenched from an elevated temperature there is a range of temperature differentials that do not result in any loss of strength then at a fairly well-defined critical temperature differential,  $\Delta T_c$ , there is a significant loss of strength, followed by further gradual decline at increasing temperature differentials. In contrast, ceramics used as refractories tend to be porous and have lower initial strengths but retain a significant fraction of that strength after quenching without showing an abrupt loss of strength. Studies of hot pressed metal particle toughened alumina matrices indicate that the composites behave in a similar manner to monolithic alumina except that the strengths are higher throughout (although only slightly in some cases) and that  $\Delta T_c$  is increased from  $200^\circ\text{C}$  to  $300^\circ\text{C}$  for alumina–5 vol% copper<sup>34</sup> and  $450^\circ\text{C}$  for alumina containing 20 vol% of coarse ( $11\text{--}12 \mu\text{m}$ ) molybdenum particles<sup>31</sup>. Other alumina–molybdenum composites (containing 20 vol% fine ( $3 \mu\text{m}$ ) particles or 10 vol% (fine or coarse) particles) also showed improvements over monolithic alumina, but not as marked as for the coarse 20 vol% composite.

A hot pressed alumina–20 vol% iron composite also showed an improvement in  $\Delta T_c$  but a composite made from the same

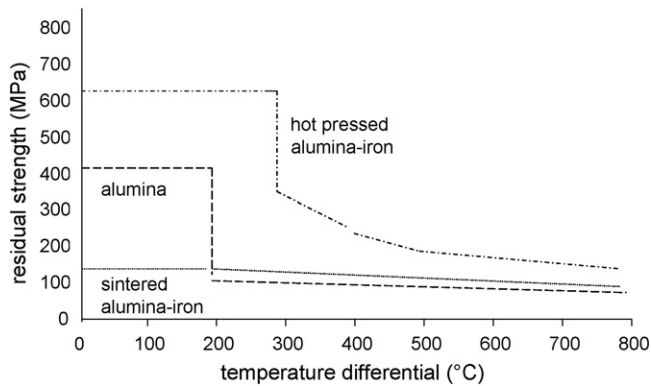


Fig. 7. Schematic showing the retained strength after quenching for alumina and two alumina–20 vol% iron composites (adapted from <sup>36</sup>).

powder blend but pressureless sintered was weaker (due to weak bonding) and behaved more like a refractory material showing a gradual loss of strength<sup>36</sup> (see Fig. 7). Modelling studies,<sup>37</sup> however, have shown that the superior behaviour of the hot pressed material was not due to the enhanced toughness but more likely to result from the reduced elastic modulus and higher thermal conductivity. A similar approach for the alumina–molybdenum composites indicated that the increased toughness for the coarse particle composite was a significant factor, although changes in the other properties did contribute to the overall thermal shock resistance.<sup>31</sup>

## 5. Outlook

Before reaching some conclusions about the future for ductile particle CMCs as structural materials, it is important to realise that this several topics have not been covered, including the changes to the electromagnetic properties resulting from the inclusion of micro- and/or nano-scale metallic particles, the potential for improving the mechanical properties of functional matrices and the development of ceramic–metal functional graded materials. All of these topics are beyond the scope of this review but are active areas of research.

Returning to the future prognosis for ductile particle CMCs as structural materials, it is clear that they do offer a unique combination of properties. Traditionally, structural ceramics are used in applications involving wear and/or high temperatures yet very few studies have looked at ductile particle CMCs under these conditions. Those that have indicate that the composites may perform better than the alumina that they would be replacing. Clearly, the microstructures have not been optimised for these situations and further work is required in this area. However, these composites suffer from the problems that beset many new materials in that the potential benefits have to outweigh the drawbacks of more difficult and hence costly processing. As yet they have not been taken into commercial applications. Hence, ductile particle ceramic matrix composites are more than scientific curiosities but not yet fully established engineering materials.

## Acknowledgements

JAY is grateful to past members of the ceramic team at the University of Surrey for providing the basis for this article. These former doctoral students were Xudong Sun, Paul Trusty, Matthew Aldridge, and Ying Ji, who were funded by the Engineering and Physical Sciences Research Council (and its forerunner, the Science and Engineering Research Council), the Committee of Vice Chancellors and Principals (ORS award), the Henry Lester Trust and Universities' China Committee and the University of Surrey. JAY is grateful to the British Council for providing funding which allowed her to visit Prof. Richard Brook during his time at the Pulvermetallurgisches Laboratorium of the Max-Planck-Institut für Metallforschung in Stuttgart. His support, encouragement and friendship since that time has been much appreciated.

## References

- Nivas, Y. and Fulrath, R. M., Limitation of Griffith flaws in glass–matrix composites. *J. Am. Ceram. Soc.*, 1970, **53**(4), 188–191.
- Rankin, D. T., Stiglich, J. J., Petrak, D. R. and Ruh, R., Hot-pressing and mechanical properties of Al<sub>2</sub>O<sub>3</sub> with an Mo-dispersed phase. *J. Am. Ceram. Soc.*, 1971, **54**(6), 277–281.
- Hing, P. and Groves, G. W., The microstructure and fracture properties of MgO crystals containing a dispersed phase. *J. Mater. Sci.*, 1972, **7**, 422–426.
- Hing, P. and Groves, G. W., The strength and fracture toughness of polycrystalline magnesium oxide containing metallic particles and fibres. *J. Mater. Sci.*, 1972, **7**, 427–434.
- Krstic, V. V., Nicholson, P. S. and Hoagland, R. G., Toughening of glasses by metallic particles. *J. Am. Ceram. Soc.*, 1981, **64**(9), 499–504.
- Krstic, V. D., On the fracture of brittle-matrix/ductile-particle composites. *Philos. Mag. A*, 1983, **48**(5), 695–708.
- Ashby, M. F., Blunt, F. J. and Bannister, M., Flow characteristics of highly constrained metal wires. *Acta metall.*, 1989, **37**(7), 1847–1857.
- Hussain, S., Barbariol, I., Roitti, S. and Sbaizero, O., Electrical conductivity of an insulator matrix (alumina) and conductor particle (molybdenum) composites. *J. Eur. Ceram. Soc.*, 2003, **23**, 315–321.
- Dlouhy, I., Reinisch, M., Boccaccini, A. R. and Knott, J. F., Fracture characteristics of borosilicate glasses reinforced by metallic particles. *Fatigue Fract. Eng. Mater. Struct.*, 1997, **20**, 1235–1253.
- Banuprakash, G., Katyal, V., Murthy, V. S. R. and Murty, G. S., Mechanical behaviour of borosilicate glass–copper composites. *Composites Part A–Appl. Sci. Manuf.*, 1997, **28**, 861–867.
- Moore, R. H. and Kunz, S. C., Metal particle-toughened borosilicate sealing glass. *Ceram. Eng. Sci. Proc.*, 1987, **8**(7–8), 839–847.
- Claxton, E., Taylor, B. A. and Rawlings, R. D., Processing and properties of a bioactive glass–ceramic reinforced with ductile silver particles. *J. Mater. Sci.*, 2002, **37**(17), 3725–3732.
- Troczyński, T. B. and Nicholson, P. S., Fracture mechanics of titanium/bioactive glass–ceramic particulate composites. *J. Am. Ceram. Soc.*, 1991, **74**(8), 1803–1806.
- Zhang, X., Gubbels, G. H. M., Terpstra, R. A. and Metselaar, R., Toughening of calcium hydroxyapatite with silver particles. *J. Mater. Sci.*, 1997, **32**, 235–243.
- Bartolomé, J. F., Díaz, M., Requena, J., Moya, J. S. and Tomsia, A. P., Mullite/molybdenum ceramic–metal composites. *Acta mater.*, 1999, **47**, 3891–3899.
- Tuan, W. H. and Brook, R. J., The toughening of alumina with nickel inclusions. *J. Eur. Ceram. Soc.*, 1990, **6**, 31–37.
- Tuan, W. H. and Brook, R. J., Processing of alumina/nickel composites. *J. Eur. Ceram. Soc.*, 1992, **10**, 95–100.

18. Breval, E., Deng, Z., Chiou, S. and Pantano, C. G., Sol–gel prepared Ni–alumina composite materials. Part 1. Microstructure and mechanical properties. *J. Mater. Sci.*, 1992, **27**, 1464–1468.
19. Breval, E. and Pantano, C. G., Sol–gel prepared Ni–alumina composite materials. Part 2. Structure and hot-pressing temperature. *J. Mater. Sci.*, 1992, **27**, 5463–5469.
20. Sun, X. and Yeomans, J. A., The toughening of alumina materials by the inclusion of nickel particles, British Ceramic Proceedings, No. 49 *Special Ceramics 9*, Institute of Ceramics, Stoke-on-Trent, UK, 1992, pp. 297–308.
21. Ekstrom, T., Alumina ceramics with particle inclusions. *J. Eur. Ceram. Soc.*, 1993, **11**, 487–496.
22. Tuan, W. H., Lin, M. C. and Wu, H. H., Preparation of Al<sub>2</sub>O<sub>3</sub>/Ni composites by pressureless sintering in H<sub>2</sub>. *Ceram. Int.*, 1995, **21**, 221–225.
23. Sun, X. and Yeomans, J., Optimization of a ductile-particle-toughened ceramic. *J. Am. Ceram. Soc.*, 1996, **79**, 2705–2717.
24. Lui, D.-M., Tuan, W. H. and Chiu, C.-C., Thermal diffusivity, heat capacity and thermal conductivity in Al<sub>2</sub>O<sub>3</sub>–Ni composite. *Mater. Sci. Eng.*, 1995, **B31**, 287–291.
25. Wang, J., Ponton, C. B. and Marquis, P. M., Silver-toughened alumina ceramics. *Br. Ceram. Trans.*, 1993, **92**, 67–74.
26. Chou, W. B. and Tuan, W. H., Toughening and strengthening with silver inclusions. *J. Eur. Ceram. Soc.*, 1995, **15**, 291–295.
27. Lui, D. M. and Tuan, W. H., Microstructure and thermal conduction properties of Al<sub>2</sub>O<sub>3</sub>–Ag composites. *Acta Mater.*, 1996, **44**, 813–818.
28. Dutta, A. K., Narasaiah, N., Chattopadhyaya, A. B. and Ray, K. K., The load dependence of hardness in alumina–silver composites. *Ceram. Int.*, 2001, **27**, 407–413.
29. Dutta, A. K., Chattopadhyaya, A. B. and Ray, K. K., Progressive flank wear and machining performance of silver toughened alumina cutting tool inserts. *Wear*, 2006, **261**, 885–895.
30. Sbaizero, O. and Pezzotti, G., Influence of residual and bridging stresses on the R-curve behavior of Mo- and FeAl-toughened alumina. *J. Eur. Ceram. Soc.*, 2000, **20**, 1145–1152.
31. Sbaizero, O. and Pezzotti, G., Influence of molybdenum particles on thermal shock resistance of alumina matrix ceramics. *Mater. Sci. Eng.*, 2003, **A343**, 273–281.
32. de Portu, G., Guicciardi, S., Melandri, C. and Monteverde, F., Wear behaviour of Al<sub>2</sub>O<sub>3</sub>–Mo and Al<sub>2</sub>O<sub>3</sub>–Nb composites. *Wear*, 2007, **262**, 1346–1352.
33. Aldrich, D. E. and Edirisinghe, M. J., Addition of copper to an alumina matrix. *J. Mater. Sci. Lett.*, 1998, **17**, 965–967.
34. Wang, L., Shi, J.-L., Lin, M.-T., Chen, H.-R. and Yan, D.-S., The thermal shock behavior of alumina–copper composite. *Mater. Res. Bull.*, 2001, **36**, 925–932.
35. Trusty, P. A. and Yeomans, J. A., The toughening of alumina with iron: effects of iron distribution on fracture toughness. *J. Eur. Ceram. Soc.*, 1997, **17**, 495–504.
36. Aldridge, M. and Yeomans, J. A., The thermal shock behaviour of ductile particle toughened alumina composites. *J. Eur. Ceram. Soc.*, 1998, **19**, 1769–1775.
37. Aldridge, M. and Yeomans, J. A., Thermal shock behaviour of iron-particle-toughened alumina. *J. Am. Ceram. Soc.*, 2001, **84**(3), 603–607.
38. Lane, S. M., Biner, S. B. and Buck, O., Room temperature fracture and high temperature creep characteristics of 20 vol% Nb particulate reinforced alumina. *Mater. Sci. Eng.*, 1998, **A246**, 244–251.
39. Ji, Y. and Yeomans, J. A., Microstructure and mechanical properties of chromium and chromium/nickel particulate reinforced alumina ceramics. *J. Mater. Sci.*, 2002, **37**, 5229–5236.
40. Sun, X. and Yeomans, J. A., Influence of particle size distribution on ductile-phase toughening in brittle materials. *J. Am. Ceram. Soc.*, 1996, **79**(2), 562–564.
41. Tuan, W. H. and Chen, W. R., The interactions between silver and zirconia inclusions and their effects on toughening behaviour of Al<sub>2</sub>O<sub>3</sub>/(Ag + ZrO<sub>2</sub>) composites. *J. Eur. Ceram. Soc.*, 1994, **14**, 37–43.
42. Tuan, W. H. and Chen, W. R., Mechanical properties of alumina–zirconia–silver composites. *J. Am. Ceram. Soc.*, 1995, **78**, 465–469.
43. Chen, R. Z. and Tuan, W. H., Toughening alumina with silver and zirconia inclusions. *J. Eur. Ceram. Soc.*, 2001, **21**, 2887–2893.
44. Lalonde, J., Scheppokat, S., Janssen, R. and Claussen, N., Toughening of alumina/zirconia ceramic composites with silver particles. *J. Eur. Ceram. Soc.*, 2002, **22**, 2165–2171.
45. Niihara, K., New design concept of structural ceramics: ceramic nanocomposites. *J. Ceram. Soc. Jpn.*, 1991, **99**, 974–982.
46. Sekino, T., Nakajima, T. and Niihara, K., Mechanical and magnetic properties of nickel dispersed alumina-based nanocomposites. *Mater. Lett.*, 1996, **29**, 165–169.
47. Sekino, T., Nakajima, T., Ueda, S. and Niihara, K., Reduction and sintering of a nickel-dispersed-alumina composite and its properties. *J. Am. Ceram. Soc.*, 1997, **80**(5), 1139–1148.
48. Chen, R. Z. and Tuan, W. H., Pressureless sintering of Al<sub>2</sub>O<sub>3</sub>/Ni nanocomposites. *J. Eur. Ceram. Soc.*, 1999, **19**, 463–468.
49. Lu, J., Gao, L., Sun, J., Gui, L. and Guo, J., Effect of nickel content on the sintering behavior, mechanical and dielectric properties of Al<sub>2</sub>O<sub>3</sub>/Ni composites from coated powders. *Mater. Sci. Eng.*, 2000, **A293**, 223–228.
50. Lieberthal, M. and Kaplan, W. D., Processing and properties of Al<sub>2</sub>O<sub>3</sub> nanocomposites reinforced with sub-micron Ni and NiAl<sub>2</sub>O<sub>4</sub>. *Mater. Sci. Eng.*, 2001, **A302**, 83–91.
51. Li, G.-J., Huang, X.-X. and Guo, J.-K., Fabrication, microstructure and mechanical properties of Al<sub>2</sub>O<sub>3</sub>/Ni nanocomposites by a chemical method. *Mater. Res. Bull.*, 2003, **38**, 1591–1600.
52. Aharon, O., Bar-Ziv, S., Gorni, D., Cohen-Hyams, T. and Kaplan, W. D., Residual stresses and magnetic properties of alumina–nickel nanocomposites. *Scr. Mater.*, 2004, **50**, 1209–1213.
53. Yao, X., Huang, Z., Chen, L., Jiang, D., Tan, S., Michel, D. *et al.*, Alumina–nickel composites densified by spark plasma sintering. *Mater. Lett.*, 2005, **59**, 2314–2318.
54. Nawa, M., Sekino, T. and Niihara, K., Fabrication and mechanical behaviour of Al<sub>2</sub>O<sub>3</sub>/Mo nanocomposites. *J. Mater. Sci.*, 1994, **29**, 3185–3192.
55. Lu, J., Gao, L., Guo, J. and Niihara, K., Preparation, sintering behavior, and microstructural studies of Al<sub>2</sub>O<sub>3</sub>/Mo composites from boehmite-coated Mo powders. *Mater. Res. Bull.*, 2000, **35**, 2387–2396.
56. Díaz, L. A., Valdés, A. F., Díaz, C., Espino, A. M. and Torrecillas, R., Alumina/molybdenum nanocomposites obtained in organic media. *J. Eur. Ceram. Soc.*, 2003, **23**, 2829–2834.
57. Sekino, T. and Niihara, K., Microstructural characteristics and mechanical properties for Al<sub>2</sub>O<sub>3</sub>/metal nanocomposites. *Nanostruct. Mater.*, 1995, **6**, 663–666.
58. Sekino, T. and Niihara, K., Fabrication and mechanical properties of fine-tungsten-dispersed alumina-based composites. *J. Mater. Sci.*, 1997, **32**, 3943–3949.
59. Guichard, J. L., Tillement, O. and Mocellin, A., Preparation and characterization of alumina–iron cermets by hot-pressing nanocomposite powders. *J. Mater. Sci.*, 1997, **32**, 4513–4521.
60. Laurent, Ch., Peigney, A., Quénard, O. and Rousset, A., Synthesis and mechanical properties of nanometric metal particles–ceramic matrix nanocomposites. *Silic. Ind.*, 1998, **63**, 77–84.
61. Guichard, J. L., Tillement, O. and Mocellin, A., Alumina–chromium cermets by hot-pressing of nanocomposite powders. *J. Eur. Ceram. Soc.*, 1998, **18**, 174–1752.
62. Ji, Y. and Yeomans, J. A., Processing and mechanical properties of Al<sub>2</sub>O<sub>3</sub>–5 vol.% Cr nanocomposites. *J. Eur. Ceram. Soc.*, 2002, **22**, 1927–1936.
63. Marcin, C. and Katarzyna, P., Processing, microstructure and mechanical properties of Al<sub>2</sub>O<sub>3</sub>–Cr nanocomposites. *J. Eur. Ceram. Soc.*, 2007, **27**, 1273–1279.
64. Oh, S.-T., Sekino, T. and Niihara, K., Fabrication and mechanical properties of 5 vol% copper dispersed alumina nanocomposite. *J. Eur. Ceram. Soc.*, 1998, **18**, 31–37.
65. Oh, S.-T., Lee, J.-S., Sekino, T. and Niihara, K., Fabrication of Cu dispersed Al<sub>2</sub>O<sub>3</sub> nanocomposites using Al<sub>2</sub>O<sub>3</sub>/CuO and Al<sub>2</sub>O<sub>3</sub>/Cu-nitrate mixtures. *Scr. Mater.*, 2001, **44**, 2117–2120.

66. Oh, S.-T., Sando, M. and Niihara, K., Preparation and properties of alumina/nickel–cobalt alloy nanocomposites. *J. Am. Ceram. Soc.*, 1998, **81**(11), 3013–3015.
67. Oh, S.-T., Sando, M. and Niihara, K., Processing and properties of Ni-Co alloy dispersed Al<sub>2</sub>O<sub>3</sub> nanocomposites. *Scr. Mater.*, 1998, **39**, 1413–1418.
68. Kaplan, W. D. and Avishai, A., Processing and microstructural control of metal-reinforced ceramic matrix nanocomposites. In *Ceramic Matrix Composites, Microstructure properties and applications*, ed. I. M. Low. Woodhead Publishing Ltd., Cambridge, UK, 2006, pp. 285–308, chapter 11.